HHS Public Access

Author manuscript

J Bone Miner Res. Author manuscript; available in PMC 2018 August 01.

Published in final edited form as:

J Bone Miner Res. 2017 August ; 32(8): 1761–1772. doi:10.1002/jbmr.3167.

Osteocytes Acidify their Microenvironment in response to PTHrP *in vitro* and in Lactating Mice *in vivo*

Katharina Jähn, PhD[1,*], **Shilpa Kelkar, DMD**[1], **Hong Zhao**[1], **Yixia Xie**[1], **LeAnn M. Tiede-Lewis, PhD**[1], **Vladimir Dusevich, PhD**[1], **Sarah L. Dallas, PhD**[1], and **Lynda F. Bonewald, PhD**[1,**]

[1]Department of Oral and Craniofacial Biology, School of Dentistry, University of Missouri-Kansas City, Kansas City, MO, 64108, USA

Abstract

Osteocytes appear to mobilize calcium within minutes in response to PTH injections and we have previously shown that osteocytes remove their perilacunar matrix during lactation through activation of the PTH type 1 receptor. Mechanisms utilized by osteocytes to mobilize calcium are unknown but we hypothesized that the molecular components may be similar to those used by osteoclasts. Here we show, using IDG-SW3 cells that ATP6V0D2, an essential component of vacuolar ATPase in osteoclasts, and other genes associated with osteoclastic bone resorption increase with osteoblast to osteocyte differentiation. Furthermore, PTHrP increases ATP6V0D2 expression and induces proton generation by primary osteocytes, which is blocked by bafilomycin, a vacuolar ATPase inhibitor. These *in vitro* proton measurements raised the question of osteocyte viability in an acidic environment. Interestingly, osteocytes, showed enhanced viability at pH as low as 5 compared to osteoblasts and fibroblasts *in vitro*. To study *in vivo* acidification by osteocytes, virgin and lactating CD1 mice on a low calcium diet were injected with the pH indicator dye, acridine orange, and their osteocyte lacuno-canalicular system imaged by confocal microscopy. Lower pH was observed in lactating compared to virgin animals. In addition, a novel transgenic mouse line with a GFP*tpz*-tagged collagen α2(I) chain was used. Instead of the expected reduction in GFP-fluorescence only in the perilacunar matrix, reduced fluorescence was observed in the entire bone matrix of lactating mice. Based on our experiments showing quenching of GFP *in vitro*, we propose that the observed reduction in GFP fluorescence in lactating mice is due to quenching of GFP by the acidic pH generated by osteocytes. Together these findings provide novel mechanistic insight into how osteocytes remove calcium from their perilacunar/pericanalicular matrices through active acidification of their microenvironment and show that osteocytes, like osteoclasts, are resistant to the negative effects of acid on viability.

Corresponding author: Lynda F. Bonewald, PhD, Indiana University, Indiana Center for Musculoskeletal health, 635 Barnhill Dr., Indianapolis, IN 46202, Phone: +1 317 278 5155, lbonewal@iu.edu.

*now working at Department of Osteology and Biomechanics, University Medical Center Hamburg-Eppendorf, 22529 Hamburg, Germany

**now working at Indiana Center for Musculoskeletal Health, Indianapolis, IN 46202

Disclosure The authors involved in this work have nothing to disclose.

Keywords

osteocytes; cells of bone; osteoclasts

Introduction

Bone is maintained during adulthood by the coordinated action of bone resorbing osteoclasts and bone forming osteoblasts. Osteocytes regulate the activity of osteoclasts through the expression of osteoprotegerin and receptor activator of nuclear factor κ-B ligand (RANKL) and negatively regulate osteoblasts through the expression of sclerostin [reviewed in [1–3]]. Osteocytes are terminally differentiated osteoblasts that became embedded into the newly formed bone matrix during bone formation. Once encased, osteocytes undergo a considerable phenotypic shift – decreasing their cell size, reducing the number of organelles and, most strikingly, developing an extensive network of dendrites. Lying within the fluid-filled lacuno-canalicular space, the global osteocyte network spans throughout the entire bone matrix governing a large surface area and connecting to neighboring cells, surface cells, and blood vessels to allow for communication and solute transport[4].

Osteocytes have been attributed with multiple roles ranging from mechanosensation to endocrine functions including regulating kidney function, hematopoiesis and fat metabolism to name a few (for review see [3]). Yet, one of the first hypothesized roles of osteocytes - termed ‘osteocytic osteolysis’ - was proposed as early as 1910, whereby it was suggested that these osteoblast-derived cells can resorb their perilacunar bone matrix in situations of high calcium demand[5]. We have recently demonstrated that lactation induces perilacunar resorption by osteocytes, leading to enlarged osteocyte lacunar area and that osteocytes express markers of bone resorption[6]. This effect was driven by the action of parathyroid hormone-related protein (PTHrP) via the parathyroid hormone 1 receptor (PTH1R) in osteocytes.

Osteoclasts are giant cells that are specialized for bone resorption. They form by fusion of hematopoietic progenitor cells upon macrophage-colony stimulating factor and RANKL stimulation. Osteoclasts lying on the bone surface seal to form a resorption pit to allow for bone removal. The hydroxyapatite of bone is demineralized by osteoclasts via acidification, whereby protons are generated intracellularly by carbonic anhydrases and transported into the sealed zone via the action of proton pumps i.e. vacuolar ATPases[7]. The organic matrix components of bone are digested by proteases such as cathepsin K[8].

We hypothesized that osteocytes must be able to acidify their microenvironment to remove calcium from their perilacunar matrix, and that the molecular mechanisms mediating this would be similar to those used in osteoclastic bone resorption. To investigate this, expression of genes associated with osteoclastic bone resorption were examined using cell lines and primary cells as models of osteoblast to osteocyte transition. Since PTHrP is known to induce osteocyte perilacunar remodeling *in vivo*, we next determined whether treatment with PTHrP could alter osteocyte expression of genes associated with osteoclastic bone resorption and whether it could induce osteocytes to acidify their microenvironment. If osteocytes can release mineral from bone by acidifying their microenvironment, we

reasoned that osteocytes must be an acid tolerant cell type. Their viability in acidic pH was therefore tested *in vitro*. To determine if osteocytes can acidify their microenvironment *in vivo*, lactating mice were injected with a pH indicator dye. Together, these *in vitro* and *in vivo* experiments support the hypothesis that in response to PTHrP, osteocytes use the 'osteoclast' proton pump to acidify their microenvironment and that this is responsible for the removal of calcium from the osteocyte perilacunar matrix during perilacunar remodeling.

Materials and Methods

Cell culture

IDG-SW3 are immortalized cells that have been previously established as a suitable *in vitro* model for osteoblast-to-osteocyte differentiation[9]. Cells were cultured on type I collagen-coated plates and dishes (rat tail type I collagen, BD Biosciences, San Jose, CA, USA) at passage 7-25 and seeded at 40,000 cells/cm^2 for experiments. Medium used was α-MEM with 10% heat inactivated fetal bovine serum (FBS), 100 U/ml penicillin/streptomycin (P/S) (all Hyclone, South Logan, UT, USA) and 50 U/ml IFN-γ for expansion (Life Technologies, Carlsbad, CA, USA). Differentiation at 37°C was started (day 0) in the absence of IFN-γ, and with the addition of 50 μg/ml ascorbic acid (Wako Chemicals, Richmond, VA, USA) and 4 mM β-glycerophosphate (Sigma-Aldrich, St. Louis, MO; USA). Osteocyte differentiation was followed for 29 days (media exchanged every 2-3 d). For PTH, PTHrP (both human 1-34 recombinant peptides from Bachem, Torrance, CA, USA) and bafilomycin (Sigma Aldrich, St Louis, MO, USA) treatments, control cells were incubated with the individual vehicle – for PTHrP: phosphate buffered saline (PBS), for bafilomycin: PBS with 0.1% dimethylsulfoxide (DMSO). The repeated PTHrP treatment experiment used IDG-SW3 cells at day 21 that were either cultured in the presence of vehicle for 7 days (vehicle), six days with vehicle and one day with PTHrP (1 d PTHrP), five days with vehicle and two days with PTHrP (2 d PTHrP), or seven days with PTHrP (7 d PTHrP).

MLO-Y4 cells (used at passages 20-40) and MLO-A5 cells were cultured as described previously[10,11] with αMEM + P/S + 2.5% FBS + 2.5% calf serum (CS, Invitrogen, Carlsbad, CA, USA) as medium for MLO-Y4 cells, and αMEM + P/S + 5% FBS + 5% CS for MLO-A5 cells. Cell densities for viability experiments were 5,500 MLO-Y4 cells/cm^2 and 2,500 MLO-A5 cells/cm^2 respectively.

SaOs2 and MC3T3 were cultured in αMEM + 10% FBS used at 130,000 cells/cm^2 for pH experiments (SaOs2), and at 10,000 cells/cm^2 for viability experiments (MC3T3). NIH3T3 and L929 cells were cultured in DMEM + 10% FBS. NIH3T3 were seeded at 130,000 cells/cm^2 (pH experiments) and at 2,500 cells/cm^2 (viability experiments). L929 cells were seeded at 10,000 cells/cm^2.

Primary long bone derived cells enriched for fibroblasts, osteoblasts, or osteocytes were isolated from adult C57Bl/6 mice as previously described[12]. Serial digestions with collagenase IA from *Clostridium histolyticum* and Ethylenediaminetetraacetic acid (EDTA) solution (Sigma Aldrich) were done. Digest fraction 1 was used for the fibroblast-enriched cell culture, fractions 3-4 were used as osteoblast-enriched, and fractions 7-9 were combined with outgrown osteocytes for the osteocyte-enriched cell culture. Seeding densities were

dependent on cell yield, for pH experiments - 20,000-67,500 cells/cm^2 and for viability experiments - 10,000 cells/cm^2.

Primary calvarial cells were isolated from 7 day-old double transgenic mice expressing DsRed fluorescent protein driven by the 3.6 kb collagen 1A1 promoter (mice generously provided by Dr. David Rowe, University of Connecticut Health Center) and expressing green fluorescent protein (GFP) driven by an 8kb Dmp1-promoter fragment[13]. Four serial digests with collagenase/trypsin solution (0.2% collagenase IA from *Clostridium histolyticum*, 0.05% trypsin in αMEM, all from Sigma Aldrich) were performed with the first three being 20 min, while the fourth being 30 min long. The second digest was used for experiments containing 30-40% DsRed-positive cells considered osteoblast-like cells and the remaining DsRed-negative cells as fibroblast-like cells. Further digests were performed but not collected – 2 collagenase/trypsin digests, followed by a total of 5 further serial digests alternating 4 mM EDTA in αMEM (30 min) with collagenase/trypsin (20 min) digestion. Finally, bone pieces were used for outgrowths on collagen-coated plates in αMEM + 5% FBS + 5% CS. Cells from outgrowths 2 and 3 were used for experiments as osteocyte-enriched.

All mice used for isolation of cells and for the lactation experiments described below were group housed in standard conditions of 23 ± 2°C temperature and a 12 h light/12 h dark cycle, and had free access to food and water. The University of Missouri at Kansas City (UMKC) animal facility is operated as a specific pathogen-free, AAALAC approved facility and animal care and husbandry meet the requirements in the Guide for the Care and use of Laboratory Animals (8th edition), National Research Council. All animal experiments were approved by the UMKC IACUC committee in accordance with relevant federal regulations and guidelines. No adverse side effects by any procedure were seen in experimental animals.

Cell viability

The percentage of live cells was quantified using the trypan blue exclusion method following previously published procedures[14]. Briefly, cells were seeded for experiments in 24-well plates and cultured in media adjusted with HCl to a specific pH (pH range 5-7.4). After 24, or 48 hours adherent and non-adherent cells were combined and counted to determine the percentage of viable and dead cells.

In vitro determination of cell-induced pH change

To determine pH change in the culture medium, the pH indicator SNARF-4F 5-(and-6)-carboxylic acid (SNARF, Life Technologies, Carlsbad, CA, USA) was used. Cells were washed with PBS and exposed to 100 nM PTHrP or vehicle in DMEM + 0.1% BSA w/o phenol red and sodium bicarbonate (pH 7.2-7.4). Change in pH was assessed using 10 μM SNARF. To block the vacuolar ATPase activity, cells were pre-treated for 1 h with 10 nM bafilomycin or vehicle. This established dose of the proton pump inhibitor has been used in numerous *in vitro* studies and does not negatively affect cell viability during the short incubation time used. SNARF fluorescence was assessed according to manufacturer's instructions by measuring emission at 590 nm using a Victor II plate reader (Perkin Elmer,

Waltham, MA, USA). Relative fluorescence was determined as percentage change compared to vehicle treatment.

Gene expression

RNA was isolated using Trizol reagent according to manufacturer's instructions (Invitrogen, Carlsbad, CA, USA). A total of 1 μg RNA was reverse transcribed using the High Capacity cDNA reverse transcription kit (Thermo Fisher Scientific, Waltham, MA USA). Real-time quantitative polymerase chain reaction (qPCR) was carried out in an ABI Step One Plus real time PCR (Applied Biosystems, Foster City, CA, USA) using 50 ng equivalent of cDNA per reaction. Pre-made TaqMan Gene Expression Assay (Applied Biosystems) primers and probes were used for the following genes - the vacuolar ATPase (ATP6V0D2 # Mm01222963_m1 and ATP6V0B # Mm01193847_g1), carbonic anhydrase 1 (CA1 # Mm01291532_m1) and 2 (CA2 # Mm00501572_m1), tartrate resistant acid phosphatase (ACP5 # Mm00475698_m1), cathepsin K (CTSK # Mm00484039_m1), and PTH1R (#Mm00441046_m1). Expression levels were based on CT values. The CT, cycle threshold, is defined as the number of cycles required for the fluorescent signal to cross the threshold or background level and gives an indication of relative abundance. β-actin (#Mm01205647_g1) was used as a housekeeping control gene, as it was not affected by treatment or differentiation.

Lactation experiments

Lactation experiments[6] were performed using two different mouse models. We used CD1 mice (purchased from Charles River Laboratories Wilmington, MA) and GFP-collagen mice on the C57Bl/6N background, carrying a transgene in which the topaz variant of green fluorescent protein (GFP*tpz*) was inserted into the mouse pro α2(I) collagen N-terminus and expression is driven by the 3.6 kb type I collagen promoter [15]. Fourteen week old female mice were allowed to become pregnant, deliver and lactate (n=4 animals for CD1 mice, n=8 animals for GFP-collagen mice)[6]. For this study, the mice were also placed on a low calcium diet to maximally enhance calcium demand (Teklad Diet TD.95027, Envigo, Houston, TX, USA) starting on the day of delivery. Age- and weight-matched virgin mice (n=4 animals for CD1 mice, n=8 animals for GFP-collagen mice) were used as a control.

Histological analysis

Femora from CD-1 and GFP-collagen mice were processed for backscatter scanning electron microscopy (BSEM) to quantify osteocyte lacunar area as previously described[6]. BSEM was used to image the osteocyte lacunae on the longitudinal mid-section bone surface in standardized areas of trabecular and cortical bone. Quantitation was done in a blinded fashion using ImageJ software (v1.49v: Wayne Rasband, National Institutes of Health) using a lower size limit of 10 μm^2 and an upper size limit of 250 μm^2.

The contralateral femur of the GFP-collagen mice was decalcified and 10 μm-thick cryosections of the longitudinal mid-section were cut and coverslip mounted with 50% glycerol / 50% PBS containing 1 mM $MgCl_2$. GFP-fluorescence was imaged by confocal microscopy using a Leica TCS SP5 II confocal microscope (Leica Microsystems, Wetzlar, Germany).

Determination of osteocyte lacunar pH change in lactating animals

Whole tibiae from CD1 lactating mice and their virgin control mice were used for these experiments. On day twelve of lactation, animals were injected intravenously with 5 mg/kg acridine orange (A9231, Sigma-Aldrich, St. Louis, MO; USA) in PBS and humanely sacrificed 35 minutes post injection. Tibiae were quickly extracted, cleaned and imaged with the anterio-medial surface down to detect the green-fluorescence (neutral pH; excitation 492 nm, emission 530 nm) and red-fluorescence (acidic pH, excitation 465 nm, emission 655 nm) of acridine orange inside the lacunar volume using a Leica TCS SP5 II confocal microscope. Lacunar acidification was quantified by measuring the integrated fluorescence density (product of mean grey value and area) using ImageJ in a blinded fashion. The criteria for inclusion of lacunae for measurement were: characteristic oval osteocyte lacunar shape and appropriate size (10-250 μm^2), obvious dye penetration into the lacunar space and absence of saturated pixels in the image. Background fluorescence was determined from the surrounding bone matrix. Corrected total cell/lacunar area fluorescence (CTCF)[16] was calculated as CTCF = Integrated density – (lacunar area × mean background fluorescence) for each channel. The ratio of red channel CTCF/green channel CTCF was determined[17].

Quantitation of GFP fluorescence in femora from virgin and lactating mice

GFP fluorescence in the proximal femoral cortex of virgin and lactating GFP-collagen mice was quantified on confocal images using ImageJ (blinded analysis). Background fluorescence was determined in image areas without bone matrix. Corrected total GFP fluorescence/area (CTCF)[16] was calculated as CTCF = Integrated density – (standardized area × mean background fluorescence).

Statistical analysis

All statistical analyses were performed using GraphPad InStat 3.06 for Windows (GraphPad Software, San Diego, CA, USA). Values are expressed as mean and standard error of the mean (SEM). A p-value of 0.05 or less was used as the criteria for statistical significance. Data normality was tested by histogram and Kolmogorov Smirnov test, Student's t-test was applied to compare two independent experimental groups. Multiple groups were analyzed by one-way ANOVA with post-hoc tests.

Results

Bone resorption related genes increase upon osteocyte differentiation

To investigate if osteocytes are capable of demineralizing bone matrix via acidification, the expression of genes involved in osteoclast-dependent bone resorption were examined in osteocytes. Osteoclasts are well known to demineralize the inorganic bone matrix by acidification and to digest the organic components of the bone matrix using proteases, such as cathepsin K, that function optimally at acidic pH. We have recently shown that the expression of components of the vacuolar proton pump, carbonic anhydrases, TRAP, and cathepsin K in osteocytes is increased specifically with lactation and that TRAP and cathepsin K expression is dependent on PTHrp via the PTH1R [6]. Therefore, we first sought to determine if the expression of these genes is increased during osteocyte differentiation

using the IDG-SW3 cell line that has been previously established as a model for osteoblast-to-osteocyte differentiation *in vitro*[15]. Fig. 1 shows that the expression of bone resorption genes is increased with osteocyte differentiation in IDG-SW3 cells. The protease cathepsin K (Fig. 1A, CTSK) and also TRAP (Fig. 1B, ACP5) were increased in osteocytes compared to the osteoblast stage at day 1, with cathepsin K being significantly increased from day 8 onwards and TRAP by day 15 post differentiation. Carbonic anhydrase 1 and 2 expression (Fig. 1C and 1D, CA1 and CA2) were significantly up-regulated by day 15 and continued to be highly expressed until day 29 of differentiation. Components of the vacuolar ATPase (Fig. 1E and 1F, ATP6V0B and ATP6V0D2) were also found to increase with osteocyte differentiation. Generally, expression of these genes tended to increase over time in culture with highest expression at day 29 (Fig. 1). Using statistical analysis, the largest significant increase from day 1 to day 29 was ATP6V0D2 with an 87-fold increase (Fig. 1F).

PTH1R expression increases with osteocyte differentiation and PTHrP increases ATP6V0D2 expression in mature osteocytes

Osteocytes express the PTH1R and are responsive to PTH and PTHrP. Here, we sought to investigate if PTH1R levels are changed during osteocyte differentiation. Fig. 2A shows that the expression of PTH1R follows a time-dependent increase with osteocyte differentiation in the IDG-SW3 cell line, with increased expression levels compared to the start of osteocyte differentiation. To mimic *in vitro* the chronic elevation of PTHrP that occurs *in vivo* with lactation, PTHrP was added to day 21 IDG-SW3 cells at the mature osteocyte stage. Seven days of continuous PTHrP exposure had a highly significant effect on the expression of the ATP6V0D2 compared to vehicle, 1 d or 2 d of treatment (Fig. 2B). ATP6V0D2 is an isoform of the d subunit in the vacuolar ATPase and has been shown to be an essential component of the proton pump that mediates extracellular acidification in osteoclast-dependent bone resorption[(18)].

PTHrP-induced acidification by osteocytes *in vitro* involves vATPase

Cell-induced acidification of culture media was investigated. Previously, SaOs2 cells were shown to acidify their culture medium upon PTH treatment[(19)]. Here, for a negative control, NIH3T3 fibroblasts were used and SaOs2 osteosarcoma cells were used as a positive control for comparison to IDG-SW3 cells and primary long-bone derived osteocytes. Cells were treated with PTHrP in the presence of the pH indicator SNARF. SNARF fluorescence in the culture medium increases with decreasing pH (Supplemental Fig. 1D). Fig. 3A shows non-responsive NIH3T3 cells, while Fig. 3B shows increased SNARF fluorescence in SaOs2 cells upon PTHrP treatment. Primary osteocytes also significantly acidified their culture medium with PTHrP treatment (Fig. 3C).

To investigate the PTHrP-dependent acidification during osteocyte differentiation, IDG-SW3 cells were used and medium acidification was determined throughout the culture period. PTHrP significantly induced acidification of the medium compared to control only at days 16 and 28, representing later stages of osteocyte differentiation (Fig. 3D).

Acidification by cells depends upon proton release via proton pumps. Here, we show that pre-incubation with bafilomycin, a proton pump inhibitor, completely blocked the PTHrP-

dependent acidification by primary osteocytes. PTHrP significantly increased proton generation which was blocked by pre-incubation with bafilomycin (Fig. 3E). This result suggests a significant role of the vacuolar ATPase in acidification of the microenvironment by osteocytes. The below-vehicle result seen with bafilomycin+PTHrP, even though not significantly different, is likely due to the bafilomycin pre-treatment lowering the baseline acidification potential of the osteocytes.

Estimation of theoretical H^+ concentration in lacuno-canalicular fluid in response to PTHrP—To estimate the potential of osteocytes *in vivo* to lower their lacuno-canalicular pH, data from the SNARF dye experiments in IDG-SW3 cells was used to estimate the number of H+ ions released by an individual IDG-SW3 cell in response to PTHrP treatment. The SNARF fluorescence readings for control and PTHrP treated IDG-SW3 cells were first converted to pH values by interpolation from a calibration curve of SNARF fluorescence against pH (see Supplemental Fig. 1D). Next, using the formula $[H^+] = 10^{-pH}$, the molar concentration of H^+ ions was determined. These values were then corrected for the media volume (0.4 ml) and divided by the number of IDG-SW3 cells (40,000) to determine the number of moles of H^+ ions for a single cell under control and PTHrP treated and control conditions. We took the difference between PTHrP treated and control to estimate that a single IDG-SW3 cell released 6.3×10^{-17} moles of H+ ions into the media in response to PTHrP stimulation. Assuming an estimated lacuno-canalicular fluid volume of 100 μm^3 (i.e. 10^{-13} l) this would equate to a molar concentration of H^+ ions in the lacuno-canalicular fluid of 6.3×10^{-4} M (see table 1 for calculations). The effects of bone fluid flow on dilution of ion concentration and the buffering capacity on bone fluid is unknown.

Osteocytes remain viable at acidic pH unlike osteoblasts and fibroblasts

If osteocytes are able to demineralize their surrounding perilacunar bone matrix by acidification, osteocytes would be bathed in a mild acidic microenvironment during lactation. We hypothesized that osteocytes can survive at low pH. To test this, experiments were performed with several established cell lines. Results were further verified using primary cells. For these experiments, IDG-SW3 cells were not used as they require differentiation for 21 days to express the mature osteocyte phenotype. At this mature stage there is extensive mineral throughout the culture which may have protected the cells from the experimental pH changes. Therefore, to represent osteocytes, the well characterized osteocyte-like cell line, MLO-Y4 was used. To represent fibroblasts we used L929 and NIH3T3 cells and to represent osteoblasts, MC3T3 and MLO-A5 cells were used. The cells were cultured in media with the pH adjusted to neutral or acidic pH values ranging from 5 to 7.4. MLO-Y4 cells showed greater viability than fibroblasts or osteoblasts after 24 h (Fig. 4A) or 48 h (Fig 4B) in acidic pH culture conditions. Furthermore, we found that primary bone cells were also affected by acidic pH (Fig. 4C). Cells derived from second digest; DsRed-negative and therefore fibroblast-like, or DsRed-positive thought to be osteoblasts, did not survive 24 h culture at pH 5. However, cells outgrown from pre-digested bone chips, considered to be osteocyte-enriched, showed significantly higher cell viability at pH 5. These experiments show that MLO-Y4 osteocyte like cells and primary osteocytes are more resistant to acidic conditions compared to osteoblasts and fibroblasts.

Decreased pH in lactating mice on low Ca^{2+} diet

To verify that acidification occurs in the osteocyte lacunae *in vivo*, the CD1 lactation model was used. This strain is characterized by large litter size, usually between 10-15 pups per litter. Calcium demand during lactation was further increased by feeding a low-calcium diet. Prior to sacrifice, animals were injected with the pH indicator acridine orange. Femora were harvested to quantitate lacunar size and tibia to assess acridine orange fluorescence. Significantly increased osteocyte lacunar size was detected in cortical and trabecular bone of lactating mice (Fig. 5A and 5B). Acridine orange fluorescence in its neutral and acidic forms were visualized in the osteocyte lacunae of the proximal tibial cortex (Fig. 5C). Quantitation according to the CTCF method, and the ratio of acidic to neutral acridine orange was calculated for virgin and lactating mice. The ratio of acidic / neutral acridine orange was increased with lactation, demonstrating a significant decrease in the osteocyte lacunar pH with calcium demand in the lactating animals compared to virgin control mice (Fig. 5D). (Background fluorescence within osteocyte lacunae seen with vehicle injection is shown in Supplemental Fig. 1A).

We had proposed to investigate osteocyte perilacunar turnover of bone matrix proteins *in vivo* utilizing a novel transgenic mouse model where the α2 chain of type I collagen was tagged with GFP*tpz*, since GFP fluorescence is observed around the osteocyte lacunae with fainter GFP expression throughout the matrix[15] (also see Fig. 6C and Supplemental Fig. 1B). These GFP-collagen mice underwent lactation for 12 days. Low litter size of 4.5 pups / litter due to C57Bl/6N background lead to an insufficient calcium demand during lactation, and therefore a non-significant increase in osteocyte lacunar area (data not shown). However, not only was a decrease in GFP fluorescence in the perilacunar matrix observed, but surprisingly, decreased GFP fluorescence throughout the bone matrix was seen with lactation and returned post-lactation (Supplemental Fig. 1B). The experiment was repeated with a low-calcium diet to increase calcium demand. Figure 6A shows the large decline in cortical bone width and smaller trabeculae in these mice. Osteocyte lacunar area was significantly increased in both cortical and trabecular bone with lactation (Fig. 6A, B). Reduction in GFP fluorescence was detected throughout the bone matrix, not just surrounding the osteocyte lacunae (Fig. 6C). The most prominent decrease in bone matrix GFP fluorescence was observed in the proximal femur in lactating mice compared to virgin controls (Fig. 6D). The mechanisms responsible for the reduction in GFP-collagen fluorescence are presently unknown but there could be several reasons. We propose that an acidic environment around the osteocyte lacunae and canaliculi is most likely responsible for this reduction in fluorescence with lactation. GFP is known to be quenched with decreasing pH (for review, see [22]), and GFP fluorescence in protein lysates of IDG-SW3 cells which express Dmp1-GFP is also sensitive to acidic pH adjustment (Supplemental Fig. 1C). This does not rule out other potential mechanisms such as the proteolytic degradation of collagen.

Discussion

Bone has long been recognized as a reservoir of calcium, however, osteocyte regulation of systemic calcium has remained controversial. Osteoclasts have been thought to be the only regulators of calcium release from the skeleton. However, under certain conditions, such as

with PTH injection, calcium can be elevated in the circulation with minutes, far too quickly for the mobilization of osteoclasts. As the osteocyte network is exposed to an enormous surface area within the bone, it has been proposed that osteocytes could be responsible for rapid removal of calcium from the skeleton[23]. As shown here and by others, the PTH1R is highly expressed in osteocytes. Mice lacking this receptor specifically in osteocytes have impaired calcium homeostasis when subjected to a low calcium diet and do not respond to secondary hyperparathyroidism[24]. It has also been shown that these same mice fail to remodel their perilacunar matrix with lactation[6]. These data support the hypothesis that osteocytes can remove calcium from their perilacunar matrix in response to calcium demanding conditions.

Whereas the mechanisms whereby osteoclasts resorb bone have been intensively studied, little is known regarding the mechanisms that osteocytes may use to remove bone. Osteocytes were shown to express many of the “osteoclast-specific” genes such as TRAP and Cathepsin K during lactation[6]. Here we present potential mechanisms whereby osteocytes can remove mineral from bone through acidification of their surrounding bone fluid and their perilacunar matrix. Osteocytes express genes associated with osteoclastic bone resorption and importantly they express the proton pump that is required to generate an acid environment necessary for removal of mineral. Also shown here, these proton pumps in osteocytes are functional and are responsible for the reduction in pH *in vitro* in response to PTHrP. Not only have we shown that osteocytes are capable of lowering the pH in their microenvironment both *in vitro* and *in vivo*, but they are also more tolerant to acidic pH and showed increased cell viability in acidic conditions compared to osteoblasts and fibroblasts. This novel finding holds the potential for future investigations determining the survival mechanisms employed by osteocytes that appear superior over other cell types.

Hypothesizing that osteocytes, like osteoclasts, can demineralize their adjacent bone matrix by acidifying their extracellular space, we first demonstrated that expression of genes associated with osteoclastic resorption increased during osteoblast to osteocyte differentiation *in vitro*. We and others have recently demonstrated that osteocytes are capable of expressing so called “osteoclast-specific” bone resorption marker genes both at the mRNA and the protein level[6,25,26]. Interestingly, osteocytes express markers associated with the bone resorption process rather than those associated with osteoclast differentiation and fusion[6]. Although the regulatory mechanisms that control osteocyte expression of bone resorption related genes are not yet defined, certain osteocyte proteins could potentially regulate these factors in an autocrine or paracrine fashion. This has been suggested by the work from Kogawa *et al.* demonstrating sclerostin regulation of carbonic anhydrase 2, an enzyme needed for proton generation, in osteocytic cells *in vitro*[27].

While osteocytes do not form specialized sealed resorption pits as osteoclasts do, the overall effect of demineralization by osteocytes could be substantial due to the large surface area governed by the osteocyte network. Here we show that osteocytes acidify their extracellular space in response to PTHrP, the hormone that is elevated during lactation. Cells of the osteoblast lineage, but not fibroblasts, were able to acidify their culture media and the strongest effect was observed with osteocytes during osteoblast-to-osteocyte differentiation in IDG-SW3 cells *in vitro*. The PTHrP induced acidification involved the activity of

vacuolar ATPase responsible for transporting protons outside of the cells as shown by inhibition with bafilomycin. Osteoclast-dependent bone resorption occurs at very low pH, with actual values ranging from pH 3 to pH 4.7 depending on the experimental setup for determination[28]. Here we estimated osteocyte-mediated acidification to generate a theoretical proton concentration of 6.3×10^{-4} M in the lacuno-canalicular fluid in response to PTHrP. This could theoretically lead to a pH as low as 3.2, however, loading-induced bone fluid flow and the buffering capacity within the lacuna would certainly modify this pH. An estimation of osteocyte-dependent acidification has been recently made by the group of Sano *et al.*, suggesting that osteocytic osteolysis occurs around pH=5.9[29]. We know that a large amount of calcium mobilization during lactation is accomplished by osteoclasts[30], yet osteocytic osteolysis seems to be inducible early during lactation ensuring initial calcium supply[31]. Moreover, in comparison to fibroblasts and even osteoblasts, osteocytes demonstrated increased survival rates at low pH. Long term viability is considered one of the characteristics of osteocytes, with osteocytes possibly being one of the longest-living cell types in the body. The death of osteocytes, whether drug-induced or due to aging, is a hallmark of bone fragility and development of osteoporosis[32,33]. It appears that osteocytes possess a high survival potential, as demonstrated by the role of the survival mechanism autophagy in these cells, whereby osteocytes seem to have a large intrinsic capacity to withstand external stress situations[34,35].

Recently, studies have provided more insight into how perilacunar matrix is removed by osteocytes. Tang *et al.* used a mouse model with a global deletion of the matrix metalloproteinase-13 (MMP13) to demonstrate that osteocytic perilacunar remodeling with lactation is impaired in the absence of MMP13[36]. Also, a role for the calcitonin receptor on osteocytes, potentially antagonizing the PTH1R, was suggested to play a role in lactation-induced osteocytic osteolysis[37]. Here, we utilized two model systems to determine *in vivo* acidification by osteocytes. A pH indicator approach was used by injecting lactating CD1 mice on low calcium diet with acridine orange. Osteocyte lacunae in whole tibiae were more acidic in lactating mice compared to their virgin controls. The GFP-collagen mice[15] mice were also used and it was found that GFP fluorescence was reduced not only in the perilacunar region, but also throughout the bone matrix in the femora of lactating mice. Since GFP fluorescence is known to be quenched by acid pH, our interpretation of these findings is that the pH in the osteocyte lacuno-canalicular system was most likely responsible for quenching the GFP-fluorescence during lactation in these animals. Fratzl and colleagues have shown that each canaliculi is no more than one micron apart in the bone[38] suggesting the potential for significant penetration of the acidified bone fluid throughout the bone matrix. This may be the reason for the reduced GFP-fluorescence in the bone matrix and not just around the osteocyte perilacunar area. However, other potential mechanisms, such as the proteolytic degradation of collagen cannot currently be ruled out.

Based on our results we propose that osteocytes, when under conditions of high calcium demand, e.g. lactation, have the ability to produce and secrete protons that lower the pH of their lacuno-canalicular fluid filled volume to enable mineral-removal of their perilacunar matrix (Fig. 7A). Figure 7B shows acid etched SEM images of osteocytes etched under shorter acid etching conditions versus longer acid etching and illustrates that the osteocyte perilacunar matrix is distinctly more sensitive to mild acid treatment and more easily

removed by acid compared to the bone matrix further away from the osteocyte. This observation supports the concept that the acidic conditions generated in osteocyte lacunae are likely sufficient for perilacunar calcium mobilization by osteocytes.

Our novel findings of acidification within the lacuno-canalicular system strongly support the hypothesis that osteocytes demineralize their perilacunar matrix during lactation by acidifying their extracellular space. This function of osteocytes to specifically lower the pH in their lacunae may be relevant to conditions other than lactation in which there is a rapid demand for calcium or a sustained stimulus for calcium release from bone such as extended immobilization or unloading, hyperparathyroidism, or metastatic bone cancers. Further knowledge of the mechanisms by which osteocytes remove calcium and bone matrix will be valuable in helping to prevent pathological bone loss.

Supplementary Material

Refer to Web version on PubMed Central for supplementary material.

Acknowledgments

This work was supported by the National Institutes of Health / National Institute on Aging (NIH/NIA) grant 1PO1AG039355 (LFB, SLD), NIH /National Institute of Arthritis, Musculoskeletal and Skin Diseases/ (NIH/NIAMS) grant PO1 AR46798 (LFB), RC2 AR058962 (LFB), R01 AR051517 (SLD) and NIH Shared Instrumentation Grant Program S10RR027668 (SLD).

Grant support: National Institutes of Health / National Institute on Aging (NIH/NIA) grant 1PO1AG039355 (LFB, SLD), NIH /National Institute of Arthritis, Musculoskeletal and Skin Diseases/ (NIH/NIAMS) grant PO1 AR46798 (LFB), RC2 AR058962 (LFB), R01 AR051517 (SLD) and NIH Shared Instrumentation Grant Program S10RR027668 (SLD).

References

1. Prideaux, M., Findlay, DM., Atkins, GJ. Curr Opin Pharmacol. Vol. 28. Elsevier Ltd; 2016. Osteocytes: The master cells in bone remodelling; p. 24-30.[Internet]
2. Bonewald LF. The amazing osteocyte. J Bone Miner Res. 2011; 26(2):229–38. [PubMed: 21254230]
3. Dallas SL, Prideaux M, Bonewald LF. The osteocyte: An endocrine cell and more. Endocr Rev. 2013; 34(5):658–90. [PubMed: 23612223]
4. Milovanovic P, Zimmermann EA, Hahn M, Djonic D, Pu K, Djuric M, Amling M, Division MS, Berkeley L, Road C, States U, Medicine F. Osteocytic Canalicular Networks: Morphological Implications for Altered Mechanosensitivity. ACS Nano. 2013; 7(9):7542–51. [PubMed: 23909715]
5. von Recklinghausen, FV. Untersuchungen uber Rachitis und Osteomalacia. Jena: Gustav Fischer; 1910.
6. Qing H, Ardeshirpour L, Divieti Pajevic P, Dusevich V, Jähn K, Kato S, Wysolmerski J, Bonewald L. Demonstration of Osteocytic Perilacunar/Canalicular Remodeling in Mice during Lactation. J Bone Miner Res. 2012; 27(5):1018–29. [PubMed: 22308018]
7. Blair HC, Teitelbaum SL, Ghiselli R, Gluck S. Osteoclastic bone resorption by a polarized vacuolar proton pump. Science. 1989; 245(4920):855–7. [PubMed: 2528207]
8. Inaoka T, Bilbe G, Ishibashi O, Tezuka K, Kumegawa M, Kokubo T. Molecular cloning of human cDNA for cathepsin K: novel cysteine proteinase predominantly expressed in bone. Biochem Biophys Res Commun. 1995:89–96.
9. Woo SM, Rosser J, Dusevich V, Kalajzic I, Bonewald LF. Cell line IDG-SW3 replicates osteoblast-to-late-osteocyte differentiation in vitro and accelerates bone formation in vivo. J Bone Miner Res. 2011; 26(11):2634–46. [PubMed: 21735478]

10. Kato Y, Windle J, Koop B, Mundy G, Bonewald L. Establishment of an osteocyte-like cell line, MLO-Y4. J Bone Min Res. 1997; 12(12):2014–23.
11. Kato Y, Boskey A, Spevak L, Dallas M, Hori M, Bonewald LF. Establishment of an osteoid preosteocyte-like cell MLO-A5 that spontaneously mineralizes in culture. J Bone Min Res. 2001; 16(9):1622–33.
12. Stern AR, Stern MM, van Dyke ME, Jähn K, Prideaux M, Bonewald LF. Isolation and culture of primary osteocytes from the long bones of skeletally mature and aged mice. Biotechniques. 2012; 52(6):361–73. [PubMed: 22668415]
13. Kalajzic I, Braut A, Guo D, Jiang X, Kronenberg MS, Mina M, Harris MA, Harris SE, Rowe DW. Dentin matrix protein 1 expression during osteoblastic differentiation, generation of an osteocyte GFP-transgene. Bone. 2004; 35(1):74–82. [PubMed: 15207743]
14. Kitase Y, Barragan L, Qing H, Kondoh S, Jiang JX, Johnson ML, Bonewald LF. Mechanical induction of PGE2 in osteocytes blocks glucocorticoid-induced apoptosis through both the ??-catenin and PKA pathways. J Bone Miner Res. 2010; 25(12):2381–92.
15. Kamel-ElSayed SA, Tiede-Lewis LM, Lu Y, Veno PA, Dallas SL. Novel approaches for two and three dimensional multiplexed imaging of osteocytes. Bone. 2015; 76:129–40. [PubMed: 25794783]
16. Burgess A, Vigneron S, Brioudes E, Labbé JC, Lorca T, Castro A. Loss of human Greatwall results in G2 arrest and multiple mitotic defects due to deregulation of the cyclin B-Cdc2/PP2A balance. Proc Natl Acad Sci U S A. 2010; 107(28):12564–9. [PubMed: 20538976]
17. Overly CC, Lee K, Berthiaumet E, Hollenbeck PJ. Quantitative Measurement of Intraorganelle pH in the Endosomal-Lysosomal Pathway in Neurons by Using Ratiometric Imaging with Pyranine. Proc Natl Acad Sci U S A. 1995; 92(8):3156–60. [PubMed: 7724533]
18. Wu H, Xu G, Li YP. Atp6v0d2 is an essential component of the osteoclast-specific proton pump that mediates extracellular acidification in bone resorption. J Bone Miner Res. 2009; 24(5):871–85. [PubMed: 19113919]
19. Barrett MG, Belinsky GS, Tashjian AH. A new action of parathyorid hormone. receptor-mediated stimulation of extracellular acidification in human osteoblast-like SaOS-2 cells. J Biol Chem. 1997; 272:26346–53. [PubMed: 9334207]
20. Schneider P, Meier Trüllinger M, Wepf RA, Müller R. Towards quantitative 3D imaging of the osteocyte lacuno-canalicular network. Bone. 2010; 47:848–58. [PubMed: 20691297]
21. Wang L, Wang Y, Han Y, Henderson SC, Majeska RJ, Weinbaum S, Schaffler MB. In situ measurement of solute transport in the bone lacunar-canalicular system. Proc Natl Acad Sci U S A. 2005; 102(33):11911–6. [PubMed: 16087872]
22. Campbell TN, Choy FYM. The Effect of pH on Green Fluorescent Protein: a Brief Review. Mol Biol Today. 2001; 2:1–4.
23. Cullinane DM. The role of osteocytes in bone regulation: Mineral homeostasis versus mechanoreception. J Musculoskelet Neuronal Interact. 2002; 2(3):242–4. [PubMed: 15758444]
24. Powell WF, Barry KJ, Tulum I, Kobayashi T, Harris SE, Bringhurst FR, Pajevic PD. Targeted ablation of the PTH/PTHrP receptor in osteocytes impairs bone structure and homeostatic calcemic responses. J Endocrinol. 2011; 209(1):21–32. [PubMed: 21220409]
25. Nakano Y, Toyosawa S, Takano Y. Eccentric localization of osteocytes expressing enzymatic activities, protein, and mRNA signals for type 5 tartrate-resistant acid phosphatase (TRAP). J Histochem Cytochem. 2004; 52(11):1475–82. [PubMed: 15505342]
26. Mandelin J, Hukkanen M, Li TF, Korhonen M, Liljeström M, Sillat T, Hanemaaijer R, Salo J, Santavirta S, Konttinen YT. Human osteoblasts produce cathepsin K. Bone. 2006; 38(6):769–77. [PubMed: 16337236]
27. Kogawa M, Wijenayaka AR, Ormsby RT, Thomas GP, Anderson PH, Bonewald LF, Findlay DM, Atkins GJ. Sclerostin regulates release of bone mineral by osteocytes by induction of carbonic anhydrase 2. J Bone Miner Res. 2013; 28(12):2436–48. [PubMed: 23737439]
28. Silver IA, Murrills RJ, Etherington DJ. Microelectrode studies on the acid microenvironment beneath adherent macrophages and osteoclasts. Exp Cell Res. 1988; 175(2):266–76. [PubMed: 3360056]

29. Sano H, Kikuta J, Furuya M, Kondo N, Endo N, Ishii M. Intravital bone imaging by two-photon excitation microscopy to identify osteocytic osteolysis in vivo. Bone. 2015; 74:134–9. [PubMed: 25624000]

30. Ardeshirpour L, Brian S, Dann P, VanHouten J, Wysolmerski J. Increased PTHrP and decreased estrogens alter bone turnover but do not reproduce the full effects of lactation on the skeleton. Endocrinology. 2010; 151(12):5591–601. [PubMed: 21047946]

31. Talmage RV, Doppelt SH, Fondren FB. An interpretation of acute changes in plasma 45Ca following parathyroid hormone administration to thyroparathyroidectomized rats. Calcif Tissue Res. 1976; 22(2):117–28. [PubMed: 1000348]

32. Tomkinson A, Reeve J, Shaw RW, Noble BS. The death of osteocytes via apoptosis accompanies estrogen withdrawal in human bone. J Clin Endocrinol Metab. 1997; 82:3128–3135. [PubMed: 9284757]

33. Weinstein RS, Nicholas RW, Manolagas SC. Apoptosis of osteocytes in glucocorticoid-induced osteonecrosis of the hip. J Clin Endocrinol Metab. 2000; 85:2907–2912. [PubMed: 10946902]

34. Jia J, Yao W, Guan M, Dai W, Shahnazari M, Kar R, Bonewald LF, Jiang JX, Lane NE. Glucocorticoid dose determines osteocyte cell fate. FASEB J. 2011; 25(10):3366–76. [PubMed: 21705669]

35. Onal M, Piemontese M, Xiong J, Wang Y, Han L, Ye S, Komatsu M, Selig M, Weinstein RS, Zhao H, Jilka RL, Almeida M, Manolagas SC, O'Brien CA. Suppression of autophagy in osteocytes mimics skeletal aging. J Biol Chem. 2013:17432–40. [PubMed: 23645674]

36. Tang SY, Herber RP, Ho SP, Alliston T. Matrix metalloproteinase-13 is required for osteocytic perilacunar remodeling and maintains bone fracture resistance. J Bone Min Res. 2012; 27(9): 1936–50.

37. Clarke MV, Russell PK, Findlay DM, Sastra S, Anderson PH, Skinner JP, Atkins GJ, Zajac JD, Davey RA. A role for the calcitonin receptor to limit bone loss during lactation in female mice by inhibiting osteocytic osteolysis. Endocrinology. 2015; 156(9):3203–14. [PubMed: 26135836]

38. Kerschnitzki M, Kollmannsberger P, Burghammer M, Duda GN, Weinkamer R, Wagermaier W, Fratzl P. Architecture of the osteocyte network correlates with bone material quality. J Bone Miner Res. 2013; 28(8):1837–45. [PubMed: 23494896]

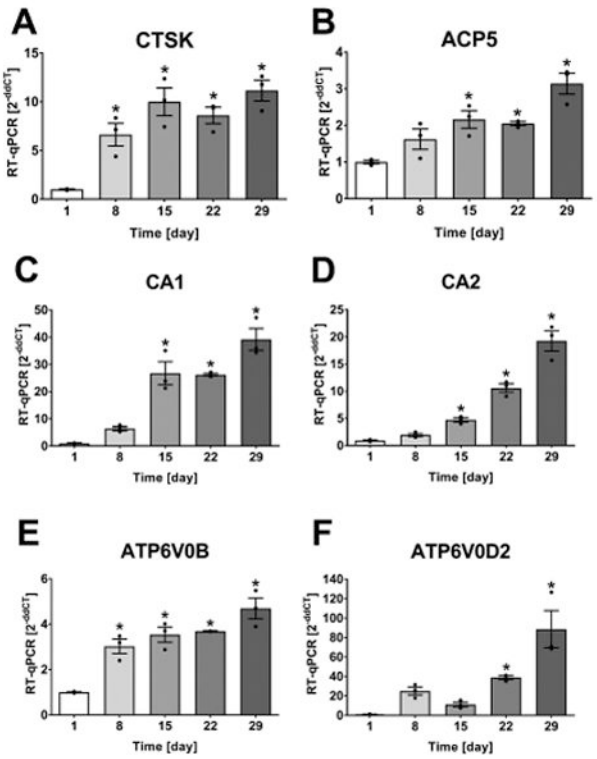

Fig. 1.

Increased expression of bone resorption related genes in osteocytes. IDG-SW3 cells were differentiated for 29 d. (A) CTSK (CT=23-21), (B) ACP5 (CT=29-28), (C) CA1 (CT=34-29), (D) CA2 (CT=32-29), (E) ATP6V0B (CT=24-23), and (F) ATP6V0D2 (CT=40-32) were significantly increased with osteocyte-differentiation. Graphs show individual data points, mean and SEM for fold change in gene expression compared to day 1 (4 experiments, representative experiment shown with n=3). Statistical analysis: one-way ANOVA and Dunnett posthoc test compared to day 1.

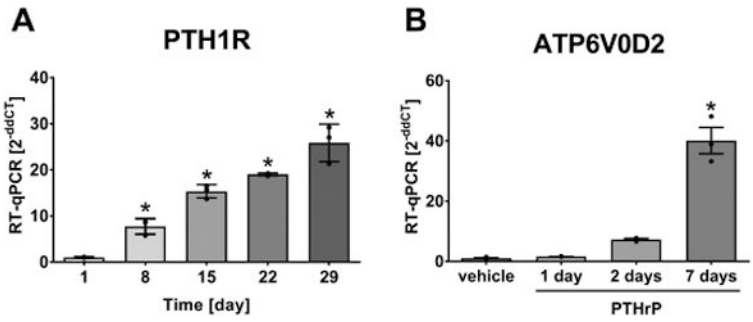

Fig. 2.

The expression of PTH1R (A) increases during osteocyte differentiation in IDG-SW3 cells (CT=25-21). PTHrP induced a further increase in ATP6V0D2 expression (CT=32-27) with a long-term treatment of 7 d (B). Graphs show individual data points, mean and SEM for fold change in gene expression compared to day 1 (4 experiments, representative experiment shown with n=3). Statistical analysis: one-way ANOVA and (A) Dunnett posthoc test compared to day 1, and (B) Tukey posthoc test comparing all groups.

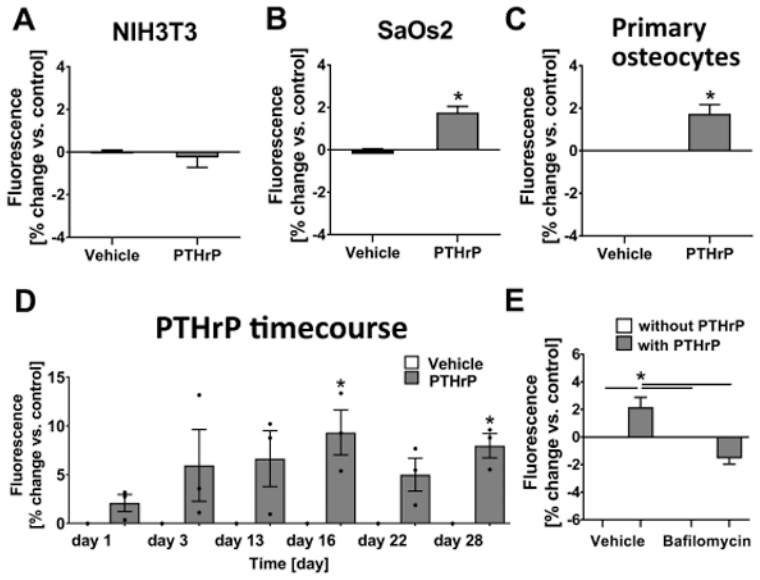

Fig. 3.

Osteocytes acidify their microenvironment *in vitro* in response to PTHrP and this is mediated by the vacuolar ATPase. Cells were treated for 20 min with PTHrP in the presence of SNARF; (A) NIH3T3 fibroblasts (8 experiments, n=3 each) did not respond to PTHrP, while (B) SaOs2 osteosarcoma cells (5 experiments, n=3-4 each) and (C) primary osteocytes (4 experiments, n=2-3 each) demonstrated significant increase in SNARF fluorescence upon PTHrP treatment (mean and SEM, unpaired two-tailed t-test compared to vehicle). (D) PTHrP-induced acidification upon osteocyte differentiation in IDG-SW3 cells (mean and SEM, 3 experiments, n=3 each, one-way; ANOVA and Bonferroni posthoc test compared to vehicle group on each day). (E) Bafilomycin blocked PTHrP-induced acidification in primary osteocytes (5 experiments, n=2-3 each, mean and SEM, one-way ANOVA and Tukey posthoc test comparing all groups).

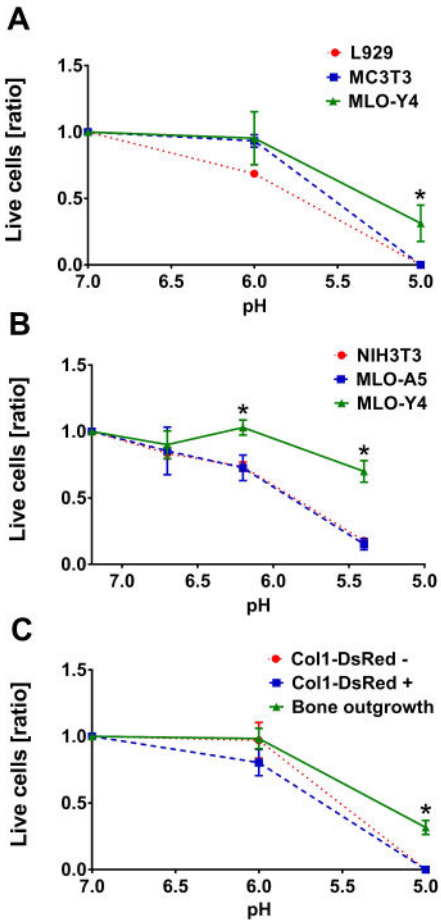

Fig. 4.

Osteocytes remain viable at low pH. Three cell types were cultured in media with adjusted pH, viability was assessed by trypan blue assay (ratio live cells / dead cells with mean and SEM). (A) MLO-Y4 cells maintained higher viability in pH 5 media at 24 h than L292 and MC3T3 (3 experiments, n=3 each, two-way ANOVA and Tukey posthoc test comparing all groups). (B) MLO-Y4 remain more viable than NIH3T3 and MLO-A5 during 48 h in media with pH≤6.5. (6 experiments, n=2-4 each, two-way ANOVA and Tukey posthoc test comparing all groups). (C) Osteocyte enriched primary calvarial cells outgrown from pre-digested bone chips showed the highest cell viability after 24 h at pH 5 compared to DsRed-negative cells and DsRed-positive cells (3 experiments, n=3 each, two-way ANOVA and Tukey posthoc test comparing all groups).

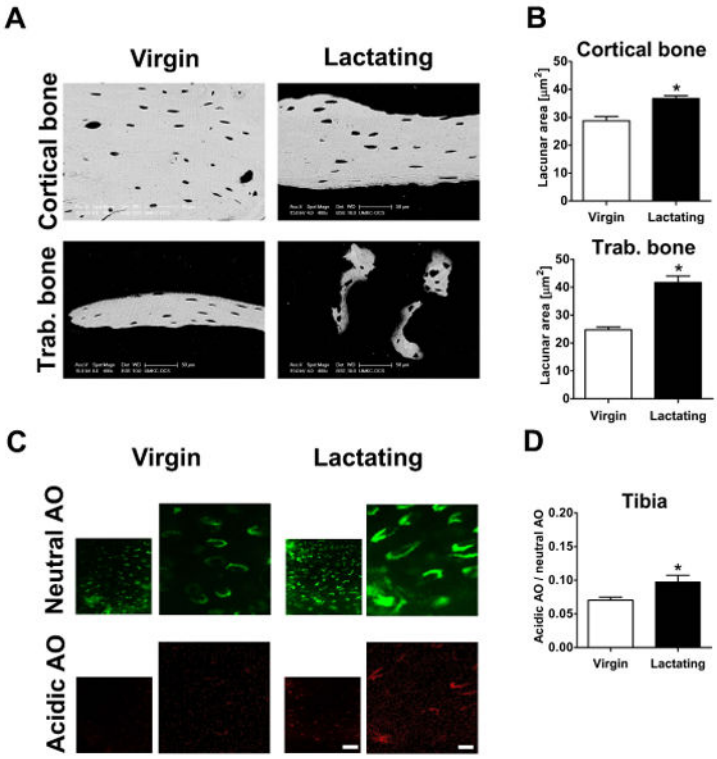

Fig. 5.

Lower pH in osteocyte lacunae of lactating mice. (A) Representative BSEM images of cortical (upper surface = periosteal, lower surface = endocortical) and trabecular bone from femora of virgin and lactating CD-1 mice. (B) Increased osteocyte lacunar area in cortical (100-300 lacunae) and trabecular (25-150 lacunae) bone in lactation group (mean and SEM, n=4 animals/group, unpaired two-tailed t-test compared to virgin). (C) Representative confocal images of acridine orange fluorescence in osteocyte lacunae in tibial cortex of virgin and lactating mice. In the left images the scale bar represents 50 µm, and in the right images, which are higher magnifications of the left the scale bar represents 10 µm. (D) Ratio of acidic to neutral AO fluorescence is significantly higher in lactating mice (mean and SEM, n=4 animals/group, 30-60 lacunae each, unpaired two-tailed t-test compared to virgin).

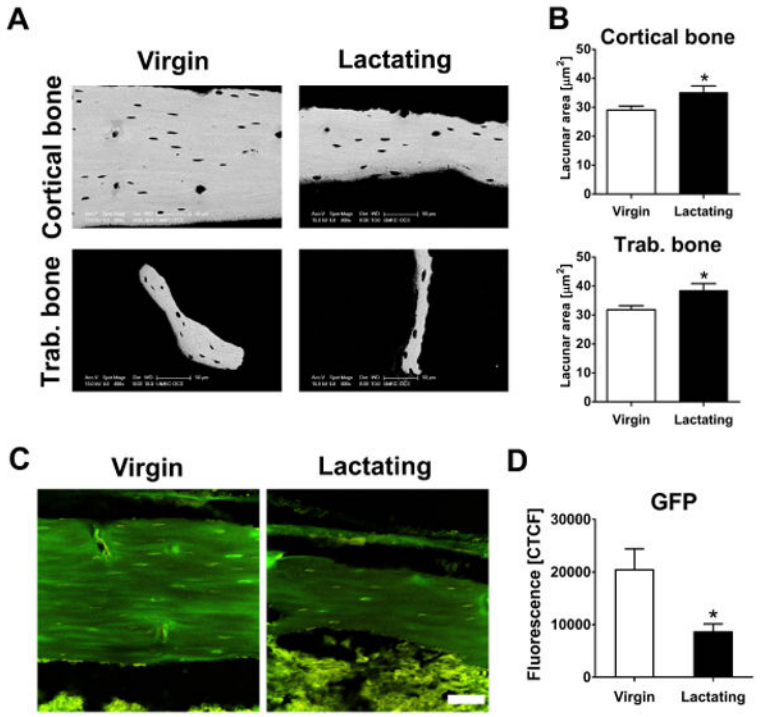

Fig. 6.

Decreased GFP fluorescence in bones of lactating GFP-collagen mice. (A) Representative BSEM images of cortical (upper surface = periosteal, lower surface = endocortical) and trabecular bone from femora of virgin and lactating GFP-collagen mice. (B) Lactation led to increased osteocyte lacunar area in cortical (125- 235 lacunae) and trabecular (25-100 lacunae) bone (mean and SEM, n=8 animals/group, unpaired two-tailed t-test comparing to virgin). (C) Representative confocal images of GFP fluorescence in the femoral cortex of virgin and lactating mice (GFP fluorescence in green, autofluorescence in yellow; scale bar = 50 μm for each image). (D) GFP fluorescence is significantly lower in cortical bone of the proximal femur of lactating mice (mean and SEM, n=8 animals/group, 4 images w/ 8 randomly assigned areas, unpaired two-tailed t-test compared to virgin).

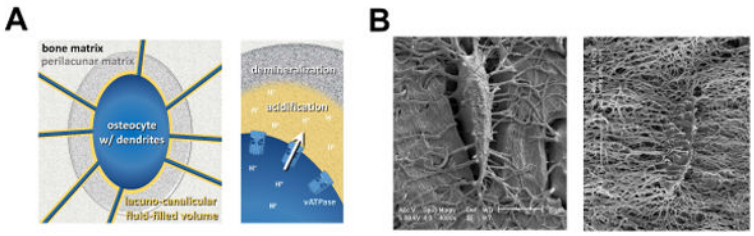

Fig. 7.

Illustration of theoretical acidification by osteocytes and visualization of the osteocyte environment. (A) Schematic image showing osteocyte with dendrites (blue) in bone (light grey) that is bathed in lacuno-canalicular fluid filled volume (yellow) and surrounded by perilacunar matrix (dark grey). (B) Representative BSEM images of acid etched murine bone specimens containing osteocyte lacuna. With short acid etching (left image) the perilacunar matrix is etched away but the removal of the neighboring and deeper bone matrix requires longer acid etching (right image).

Table 1

Values used for theoretical *in vivo* lacuno-canalicular proton concentration by osteocytes upon exposure to PTHrP.

	Parameter	Dimension
1)	40,000 IDG-SW3 cells in 400 µl medium (10 min medium acidification):	
	pH for vehicle	7.37 (c[H^+] = 0.427 nM)
	pH for 100 nM PTHrP	7.31 (c[H^+] = 0.490 nM)
	n[H^+] for 1 cell (vehicle)	4.27×10^{-16} mol
	n[H^+] for 1 cell (PTHrP)	4.90×10^{-16} mol
	H^+ released by 1 cell due to PTHrP	**6.3×10^{-17} mol** ($4.90\times10^{16} - 4.27\times10^{16}$)
2)	volume of lacuna	250 µm^3
	volume of cell	200 µm^3
	lacunar fluid-filled volume	**50 µm^3** (250 µm^3 − 200 µm^3)
	length of dendrite	25 µm
	diameter dendrite	100 nm
	diameter of canaliculi	250 nm
	volume of canalculi	60 µm^3 (1.2 µm^3 × 50 dendrites)
	volume of dendrite	10 µm^3 (0.2 µm^3 × 50 dendrites)
	canalicular fluid-filled volume	**50 µm^3** (60 µm^3 − 10 µm^3)
	lacuno-canalicular fluid-filled volume	**100 µm^3 = 10^{-13} l** (50 µm^3 + 50 µm^3)
3)	c [H^+] released by 1 cell *in vivo*	6.3×10^{-4} M (6.3×10^{-17} mol / 10^{-13} l)